NASA TECHNICAL NOTE

ESTIMATING THERMAL CONDUCTIVITY OF CERMET FUEL MATERIALS FOR NUCLEAR REACTOR APPLICATION

by John V. Miller

Lewis Research Center
Cleveland, Ohio
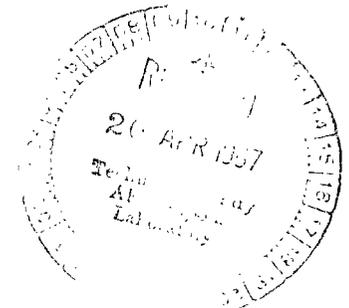
ESTIMATING THERMAL CONDUCTIVITY OF CERMET FUEL MATERIALS

FOR NUCLEAR REACTOR APPLICATION

By John V. Miller

Lewis Research Center
Cleveland, Ohio

NATIONAL AERONAUTICS AND SPACE ADMINISTRATION

ESTIMATING THERMAL CONDUCTIVITY OF CERMET FUEL MATERIALS

FOR NUCLEAR REACTOR APPLICATION

by John V. Miller

Lewis Research Center

SUMMARY

One of the parameters that must be known to determine the operating temperature of fuel elements in a nuclear reactor is the thermal conductivity of the material. When the material is a cermet (ceramic fuel particles embedded in a matrix of metallic material), the determination of the thermal conductivity without extensive experimentation is difficult because of the complex nature of the heat conduction process in such a material.

Several analytical methods that can be used to predict the conductivity in such systems were examined, and each was found to be valid over certain ranges. Some of the work being done on cermet fuels, however, is in a region that is not specifically covered by any of the models. Because of the similarity between two of the analytical models, a method that, in essence, allows extrapolation into this undefined region is suggested. Comparison with available experimental values shows that the suggested method results in favorable predictions and could, therefore, be used to estimate the thermal conductivity of potential cermet fuel materials.

Data were then generated by this method to illustrate the thermal conductivity behavior of a typical cermet fuel (tungsten - uranium dioxide) under various conditions.

INTRODUCTION

To establish the operating temperature of the fuel elements in a nuclear reactor, it is necessary to know the neutron flux distribution, the coolant flow rate and temperature, the heat-transfer coefficient, the fuel-element geometry, and the physical properties of the material that influence the temperature under both steady-state and transient conditions. Among the properties, the thermal conductivity of the material is essentially the controlling factor in determining the difference between the fuel-element surface temperature T_w and the maximum ("centerline") temperature T_{max} existing within the mate-

rial during steady-state operation. Equation (1) expresses this temperature difference for a simple, one-dimensional, flat-plate geometry in which the thermal conductivity is independent of temperature:

$$T_{max} - T_w = \frac{QL^2}{8K} \tag{1}$$

For a constant heat generating rate Q and plate thickness L, the temperature difference is inversely proportional to the thermal conductivity of the fueled material K. When a fuel element is operating near its maximum allowable temperature, based on either mechanical or metallurgical considerations, it becomes extremely important to establish the thermal conductivity of the material.

Many fuel elements are made by melting two or more metals into a composite in which the fuel material is homogeneously alloyed with the other metals. In such alloys the mechanism of heat transfer by conduction is relatively simple, and the thermal conductivity of the composite alloy can be experimentally determined with the same techniques that are used for pure metals. In general, the thermal conductivity of the alloy at a given temperature is only a function (not necessarily linear) of the relative amounts of the various constituents contained in the composite, and the conductance of such a system can be determined by a minimum number of experimental points.

However, in a cermet fuel element, in which the heat-generating material consists of individual ceramic particles heterogeneously dispersed within a metallic matrix, the heat conduction process is more complex than in that of an alloy system. The thermal conductivity of the fuel element is dependent upon the size, shape, and orientation of the particles as well as the relative amounts and properties of the materials used.

While it is possible to obtain measurements of the effective thermal conductivity of cermets by the same techniques used for alloys, extrapolation to points that are not coincidental with those determined experimentally is difficult because of the additional variables (i.e., particle size, shape, and orientation) associated with the cermets. During the early phases of a reactor design project, a reliable method of predicting the thermal conductivity will allow a detailed thermal analysis of the reactor core to be conducted long before the final fuel loading, composition, and manufacturing procedures for the cermet fuel elements have been established. It becomes important, therefore, to understand more fully the exact nature of the conduction process for such materials in order that estimation of the thermal conductivity of potential fuel element material can be made.

The purpose of this study is to investigate analytical methods of predicting thermal conductivity of cermets and to evaluate such methods by comparison with available experimental results. Much of the work presented here was taken from an earlier report (ref. 1). Of necessity, certain material has been omitted. Some additional data have also been added.

2

ANALYTICAL METHODS FOR PREDICTING THERMAL CONDUCTIVITY
OF CERMET FUELS

In conjunction with the study of electrical conductivity and dielectric constants, the problem of predicting the properties of heterogeneous materials has been treated mathematically by a variety of investigators. Much of this work has been summarized by Powers (ref. 2) and indicates that there are several models which appear to be suitable for estimating the thermal conductivity of cermets.

The fuel element materials of interest for nuclear reactor application are generally characterized by a fuel particle of low conductivity dispersed in a metallic matrix of a somewhat higher thermal conductivity (e.g., uranium dioxide (UO_2) or uranium nitride (UN) dispersed in tungsten, molybdenum, stainless steel, or zirconium). Therefore, only those models in which the thermal conductivity of the matrix is greater than that of the particle $K_m > K_p$ were considered. (Symbols are defined in appendix A.)

Basic Models

If a small number of spherical particles are dispersed into another material, it is possible to derive a mathematical equation for the mean or effective conductivity of the composite material in terms of the volume fraction of the particles and the conductivity of the two constituent materials. Representative of numerous such expressions is the Rayleigh-Maxwell dilute dispersion equation (ref. 2, p. 7):

$$K_{eff} = K_m \left[\frac{2K_m + K_p - 2V_p(K_m - K_p)}{2K_m + K_p + V_p(K_m - K_p)} \right] \tag{2}$$

where K_{eff} is the effective conductivity of the composite.

Powers (ref. 2) notes that this model has been successfully applied to such diverse materials as metals, petroleum products, paints, and blood. Because of the assumptions made in the derivation of this model, however, equation (2) is only applicable for dilute dispersions, where the particle concentration is less than 10 to 15 volume percent (ref. 2, p. 26). A more general equation for a variable dispersion of spheres has been derived by Bruggeman (ref. 2, p. 10) and should be applicable for any concentration. The form of the equation for this model is given by equation (3) and was developed by first differentiating the Rayleigh-Maxwell equation (eq. (2)) and then integrating between the appropriate limits:

$$K_{eff} = K_p + (1 - V_p)(K_m - K_p)\left(\frac{K_{eff}}{K_m}\right)^{1/3} \qquad (3)$$

Actually, this model could only apply to a particle concentration of no more than 74.05 volume percent, because this is the maximum packing density for spheres stacked in a rhombohedral array (ref. 3). Beyond this concentration or for lesser concentrations in which the particles are not uniformly distributed, a more suitable model is an equation such as another derived by Bruggeman (ref. 2, pp. 9 to 10). This equation applies to the
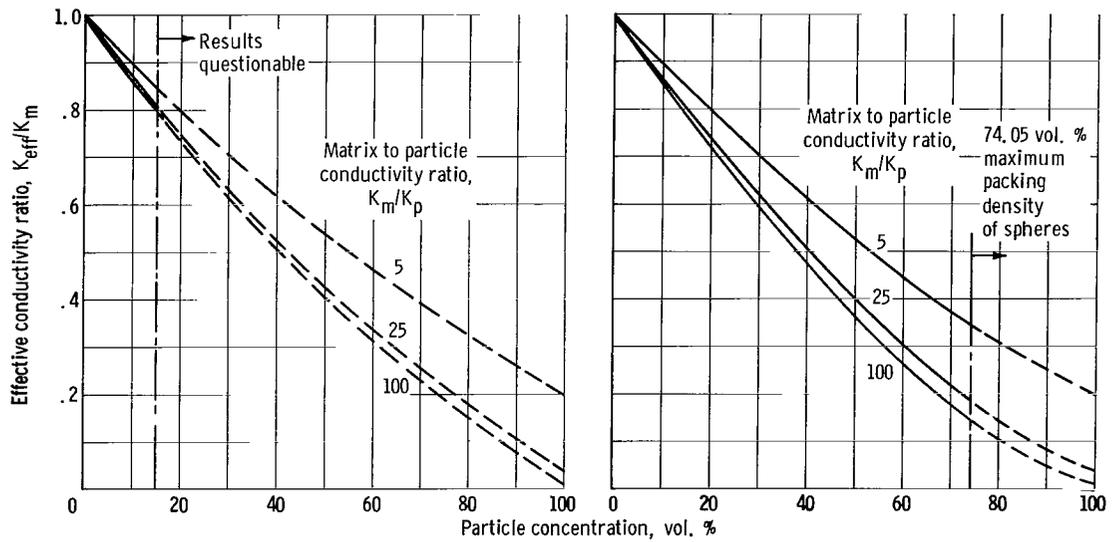
(a) Rayleigh-Maxwell dilute dispersion (see eq. (2)).

(b) Bruggeman variable dispersion (see eq. (3)).
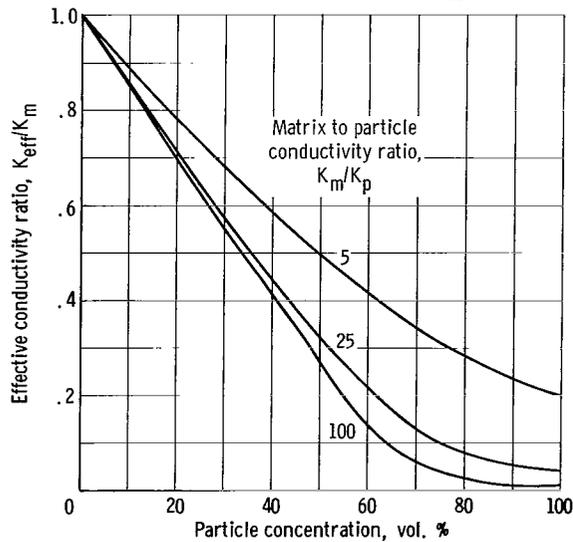
(c) Bruggeman mixture model (see eq. (4)).

Figure 1. - Conductivity of dispersion and mixtures.

so-called mixtures where neither phase is completely surrounded by the other phases:

$$\frac{K_m - K_{eff}}{K_m + 2K_{eff}} = \frac{V_p}{1 - V_p} \frac{K_{eff} - K_p}{2K_{eff} + K_p} \qquad (4)$$

Figure 1 shows the results of applying these three models (eqs. (2), (3), and (4)) to a series of cases where the ratio of the matrix to particle conductivity (K_m/K_p) was 5, 25, and 100. The solid portion of the curves represents the region where the model applies, while the dashed portion of the curves is beyond the recommended range of the model - 15 volume percent for the dilute dispersion model (eq. (2)) and 74.05 volume percent for the variable dispersion model (eq. (3)).

Basically, there is little difference between the results obtained with the three models when the particle concentration is low. This is evident from figure 2, where the three models are compared for a base material conductivity ratio (K_m/K_p) of 50. Up to a particle concentration of about 30 volume percent, the deviation between the three models is less than 10 percent. At higher concentrations, the results deviate considerably. It should be noted, however, that even at a particle concentration of 50 volume percent, the difference between the dilute dispersion model (eq. (2)) and the variable dispersion model (eq. (3)) is only about 10 percent. Because these conditions are actually beyond the recommended limits of the dilute dispersion equation ($>$15 volume percent), the absolute value of the error is academic and is only important in establishing the areas where similarity between the two methods would allow the use of either model with a minimum error. The use of this similarity will be discussed in the next section.
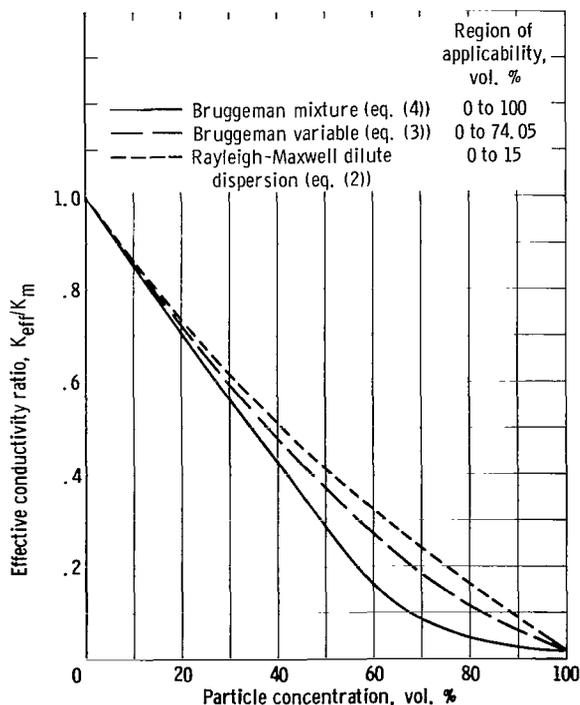
Anisotropic Effects

The models described in the previous section (eqs. (2), (3), and (4)) are somewhat idealized because they are derived for materials in which the dispersed particles are spherical and the behavior is isotropic in nature. Many materials do not always behave in this ideal manner; frequently, the particles
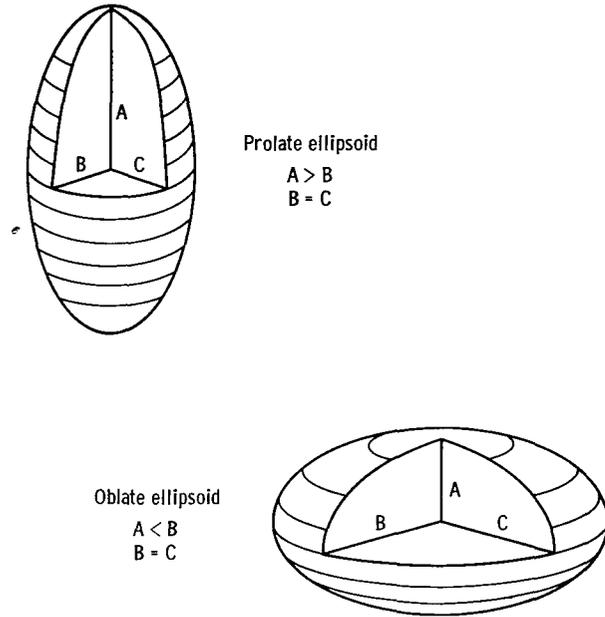

Figure 2. - Comparison of predicted conductivity. Matrix to particle conductivity ratio, 50.

Prolate ellipsoid
A > B
B = C

Oblate ellipsoid
A < B
B = C

Figure 3. - Particle shapes used in anisotropic analysis.

are distorted because of certain steps in the manufacturing process (e.g., rolling a material tends to elongate the particles), and the resulting properties are not isotropic as the previous models assumed.

Some work has been done on the anisotropic effects of such particles. A discussion of the various models is given in reference 2 (pp. 12 to 23), and the conclusion reached is that, for mathematical treatment, all particles can be classified as either prolate ellipsoids (axes A > B = C) or oblate ellipsoids (axes A < B = C), or, as they are also called, spheroids (fig. 3). Anisotropic effects are simulated by changing the relative size and orientation of the axes of the ellipsoids with respect to the direction of heat flow in the material.

Of the various anisotropic models described in reference 2, the one that seems most applicable to the dispersion fuel problem is the method of Fricke (ref. 2, pp. 18 to 21). The equation describing this model is

$$K_{eff} = K_m \left[\frac{XK_m + K_p - XV_p(K_m - K_p)}{XK_m + K_p + V_p(K_m - K_p)} \right] \tag{5}$$

where

$$X = \frac{K_m + K_p(\beta - 1)}{K_p - K_m(\beta + 1)} \tag{6}$$

and β is a function of particle shape and orientation. (The formulation of the Fricke model and the associated function β for various conditions is given in appendix B.)

In the limit, as the particles become spherical in shape (i.e., for X = 2), the model (eq. (5)) reduces to the Rayleigh-Maxwell dilute dispersion equation (eq. (2)). In the other extreme (i.e., as the prolate ellipsoids approach long cylinders, or the oblate ellipsoids approach thin platelets in shape), this equation reduces to the appropriate model, several of which are discussed in reference 2.

An anisotropic correction factor is defined as the ratio of the effective conductivity predicted by the Fricke model to that predicted by the dilute dispersion model:
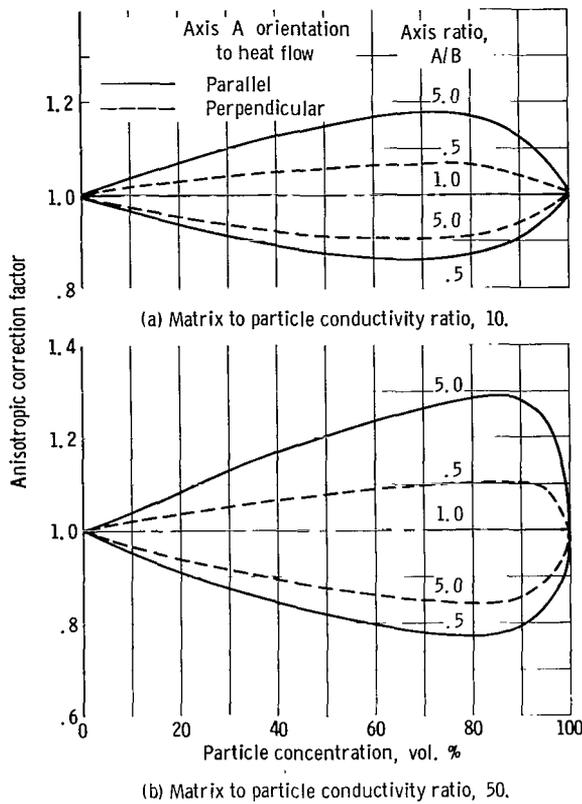
Figure 4. - Variation of the anisotropic correction factor with several parameters.

Axis A orientation to heat flow
— Parallel
— — — Perpendicular

Axis ratio, A/B

(a) Matrix to particle conductivity ratio, 10.

(b) Matrix to particle conductivity ratio, 50.

Particle concentration, vol. %

Anisotropic correction factor

$$\text{Anisotropic correction factor} = \frac{K_{(5)}}{K_{(2)}} \qquad (7)$$

where the numerical subscripts refer to the values obtained from equations (2) and (5). Figure 4 shows the result of applying this definition to several cases.

For the variable dispersion model (eq. (3)), the formulation of an anisotropic equation similar to equation (5) is not practical because, according to Powers (ref. 2), the functions "vary with composition as well as with ellipsoidal shape and orientation and so, the mathematics would be extremely difficult." When the elongation of the particle becomes extreme and when the particle concentration is high enough so that contact of adjacent particles occurs, an anisotropic model of the Bruggeman mixture equation (eq. (4)) can be derived (ref. 2, p. 21). The generalized equation for the mixture model, including anisotropic effects of particle shape and orientation, is given by

$$\frac{K_m - K_{eff}}{K_m + XK_{eff}} = \frac{V_p}{1 - V_p} \frac{K_{eff} - K_p}{XK_{eff} + K_p} \qquad (8)$$

where X is given by equation (6). As the value of X varies from zero to infinity, equation (8) represents the equation for models ranging from series laminates, X = 0, through spherical particles, X = 2, to parallel cylinders, X = ∞.

As already noted, when the particle concentration exceeds 10 to 15 volume percent, the applicability of the dilute dispersion model (eqs. (2) and (5)) is questionable. A similar situation, although not as well defined, occurs with the mixture equation (eq. (8)) when particles are not sufficiently elongated nor of sufficient concentration to cause interaction (contact) between particles.

The question that arises then is how to treat those cermet materials having nonspherical particles with concentrations greater than those allowed by the dilute model (eq. (5)) and less than that required to justify the use of the mixture model (eq. (8)).

Because of the similarity in the results obtained (fig. 2) with the dilute dispersion equation (eq. (2)) and the variable dispersion equation (eq. (3)) for spherical particles, it appears conceivable, if not probable, that such a relation would also exist if an anisotropic version of the variable dispersion model were available. It is suggested that the following method be used to determine the effective thermal conductivity of anisotropic dispersions which fall in the range where the other models are not applicable:

(1) Calculate the effective thermal conductivity of the material by using the variable dispersion model (eq. (3)) and by assuming that the particles are spherical.

(2) Calculate an anisotropic correction factor (eq. (7)) by using the ratio of the conductivities predicted by equations (2) and (5).

(3) Determine the corrected, anisotropic conductivity of the material by multiplying the value obtained from equation (3) with the anisotropic correction factor:

$$K_{eff(corrected)} = K_{(3)} \frac{K_{(5)}}{K_{(2)}} \tag{9}$$

This method (eq. (9)), in essence, makes the assumption that the anisotropic behavior of a variable dispersion model would be similar to that of the dilute dispersion model and results in a thermal conductivity that can be expressed as the variable dispersion value times a correction factor. Application of this method to some experimental data is shown in the section COMPARISON WITH EXPERIMENTAL RESULTS.

Because the formulation of this method (eq. (9)) is somewhat deductive rather than strictly mathematical (i.e., based on the similarity between the dilute and variable dispersion models), the use of the mixture equation (eq. (8)) to predict the anisotropic behavior of dispersions in this region might be considered even though it is outside the range where the mixture model is directly applicable. To ascertain the validity of such a consideration, a typical set of calculations was performed by using the mixture model and the suggested model (eq. (9)). The results (fig. 5) indicate that under isotropic conditions (spherical particles) the difference between the thermal conductivity predicted by the two methods is less than 10 percent up to particle concentration of about 40 volume percent (fig. 5(a)). However, when elongation of the particle occurs (B/A = 4), the difference between the two methods increases to nearly 75 percent at the same composition (40 vol. %). If, in the following sections, agreement is shown to exist between the suggested method (eq. (9)) and the experimental data, it follows that the use of the mixture model (eq. (8)) could not produce the same agreement and, hence, should not be used over this same range.
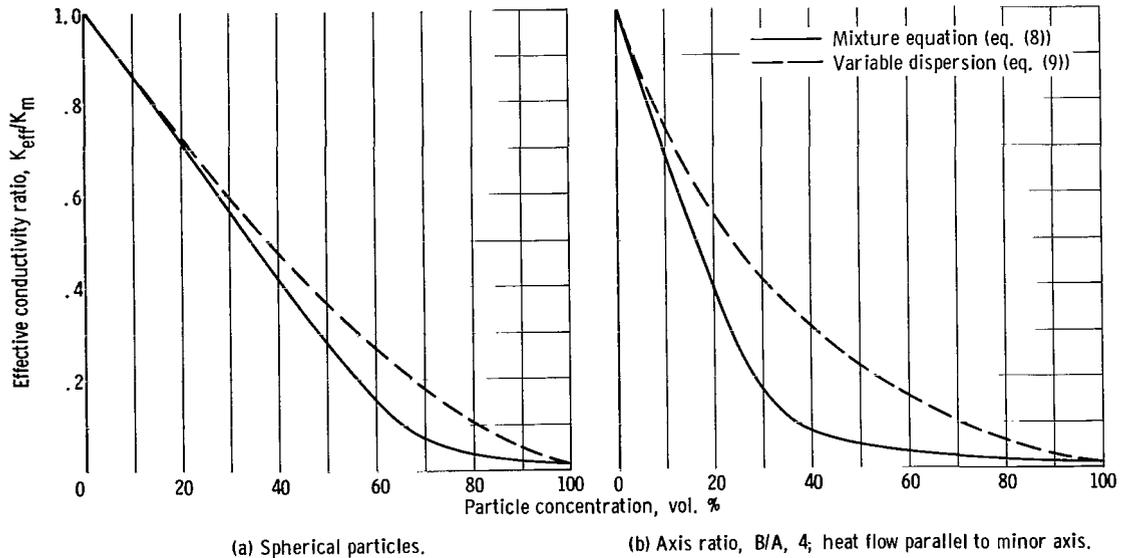
8

(a) Spherical particles.　　　　　(b) Axis ratio, B/A, 4; heat flow parallel to minor axis.

Figure 5. - Comparison of effective thermal conductivity predicted by different models. Matrix to particle conductivity ratio, 62.

Coated Particles

Kerner (ref. 2, pp. 23 to 25) derived a mathematical solution to the problem of predicting the conductivity of dispersion materials in which the particles were coated by another material. The resulting equation describing the effective thermal conductivity of a material with spherical particles p, coated with material c, and dispersed in a matrix m is given by

$$K_{eff} = \frac{K_m V_m + K_p V_p \gamma_{p,m} + K_c V_c \gamma_{c,m}}{V_m + V_p \gamma_{p,m} + V_c \gamma_{c,m}} \tag{10}$$

where the ratios of the mean field strength are

$$\gamma_{p,m} = \frac{9 K_m K_c}{(K_p + 2K_c)(K_c + 2K_m) + 2\left(\dfrac{V_p}{V_p + V_c}\right)(K_m - K_c)(K_c - K_p)}$$

and

9

$$\gamma_{c,m} = \frac{3K_m(K_p + 2K_c)}{(K_p + 2K_c)(K_c + 2K_m) + 2\left(\dfrac{V_p}{V_p + V_c}\right)(K_m - K_c)(K_c - K_p)}$$

and where $V_m + V_p + V_c = 1$.

While this coating model (eq. (10)) is only applicable to dispersions containing spherical particles, the same approach is suggested that was used in equation (9) to obtain a suitable correction factor that permits extrapolation to otherwise undefined regions. In the limit, that is, as the volume of the coating V_c decreases to zero, it can be shown that equation (10) reduces to the dilute dispersion equation for spheres (eq. (2)). Because of this fact, the coating correction factor can be defined in the same manner as the anisotropic correction factor (eq. (7)) was defined in the preceding section:

$$\text{Coating correction factor} = \frac{K_{(10)}}{K_{(2)}} \tag{11}$$

where the subscripts denote the values obtained by using equations (2) and (10).

The suggested model for anisotropic material containing coated particles then becomes

$$K_{eff} = K_{(3)}\left[\frac{K_{(5)}}{K_{(2)}}\right]\left[\frac{K_{(10)}}{K_{(2)}}\right] \tag{12}$$

which is the thermal conductivity of the variable dispersion model (eq. (3)) modified by the appropriate correction factors.

Regions of Applicability

To define exactly where each of the analytical models described in the preceding sections is applicable would be impossible because there are several areas where overlapping occurs and where the boundaries are not clearly defined. The bar graph shown in figure 6 summarizes the various regions of concern and lists the equation which applies to each. The suggested models (eqs. (9) and (12)) cover the region not presently included by the other equations; the upper limit for these suggested models was arbitrarily chosen at a particle concentration of 50 volume percent. At this concentration, the
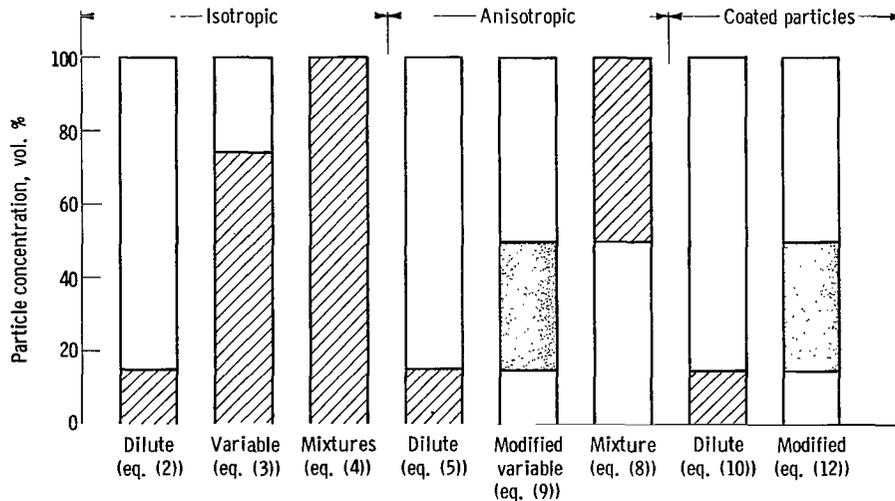
Figure 6. - Regions of applicability of equations for predicting thermal conductivity of cermet fuels. Upper limit of modified equations (eqs. (9) and (12)) arbitrarily chosen as 50 volume percent.

difference between the dilute dispersion model and the variable dispersion model was still about 10 percent (fig. 2).

# COMPARISON WITH EXPERIMENTAL RESULTS

Conductivity of Base Materials

To validate the analytical methods for predicting the thermal conductivity of cermet fuels, a literature survey was made to gather experimental results which could be compared with the predicted values. At present, the quantity of available data on the thermal conductivity of cermets is quite small. However, enough data were found to permit a cursory comparison of the analytical method.

The available data on the thermal conductivity of cermet fuels include information on tungsten - uranium dioxide (U-UO_2) dispersions (refs. 4 and 5) and on molybdenum - uranium dioxide (Mo-UO_2) dispersions (ref. 6). To compare the results of these experiments with the analytical methods, the conductivity of the base materials (i.e., W, Mo, and UO_2) must be established.

Values for the thermal conductivity of tungsten can be found in references 7 to 11. The compilation of these data is shown in figure 7(a) and, except for the room temperature region, indicates good agreement among the various sources.
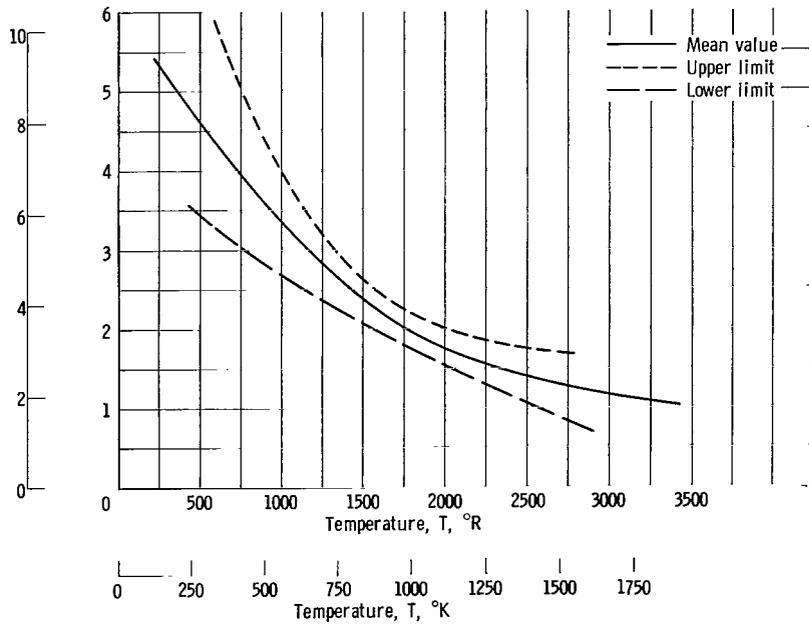
Thermal conductivity of molybdenum was taken from references 11 to 14 and is shown in figure 7(b). Data on the thermal conductivity of uranium dioxide from various sources
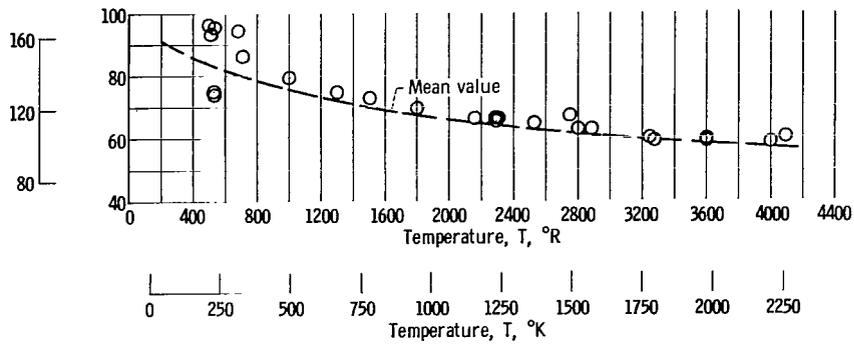
(a) Tungsten (data from refs. 7 to 10).
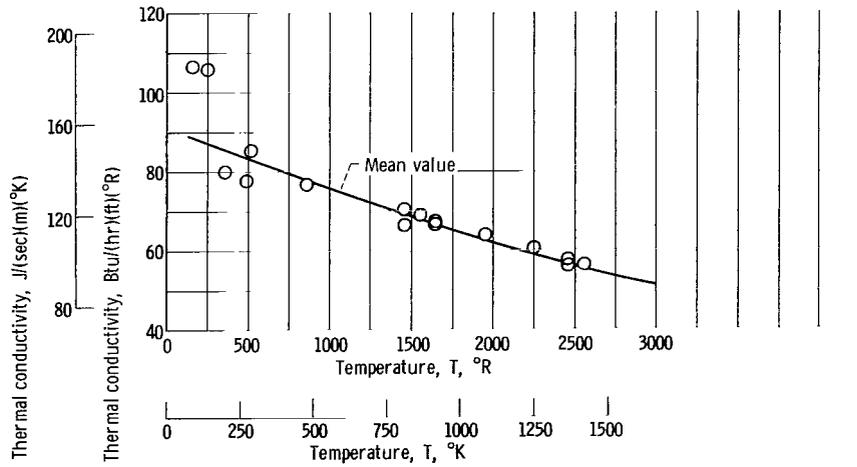
(b) Molybdenum (data from refs. 11 to 14).

(c) Uranium dioxide (limits based on refs. 15 and 16).

Figure 7. - Thermal conductivity of base materials used in typical cermet fuels.

12

has been compiled by Cottrell (ref. 15) and Belle (ref. 16). The results are summarized by establishing the upper and lower limit lines shown in figure 7(c). The wide scatter in the data can probably be attributed to the stoichiometric and density variations of the materials used by the different investigators.

It was found that a reasonable mean value fit of the data for all three materials can be expressed by an equation of the form

$$K = a - b\left(\frac{T}{10^3}\right) + c\left(\frac{T}{10^3}\right)^2 \tag{13}$$

Table I lists the value of the coefficients (a, b, and c) and approximate temperature range for tungsten, molybdenum, and uranium dioxide in both the British and the International System of units. The mean value thermal conductivity of the base materials (fig. 7) were used to compare the effective conductivity predicted by the analytical models with the available experimental data.

TABLE I. – CURVE FIT COEFFICIENTS FOR MEAN VALUE THERMAL CONDUCTIVITY

OF TUNGSTEN, MOLYBDENUM, AND URANIUM DIOXIDE

$$\left[K = a - b\left(T/10^3\right) + c\left(T/10^3\right)^2\right]$$

Material	Coefficient, Btu/(hr)(ft)($^\circ$R)			Approximate temperature range, $^\circ$R	Coefficient, J/(m)(sec)($^\circ$K)			Approximate temperature range, $^\circ$K
	a	b	c		a	b	c	
Tungsten	98.0	27.48	5.98	T < 1600	169.54	85.57	33.51	T < 890
	77.35	5.0	----	T ≥ 1600	133.82	15.57	-----	T ≥ 890
Molybdenum	91.67	16.75	1.08	500 ≤ T ≤ 3000	158.59	52.16	6.05	280 ≤ T ≤ 1670
Uranium dioxide	6.02	3.03	0.45	T < 3240	10.41	9.44	2.52	T < 1800
	1.0	-----	----	T > 3240	1.73	-----	-----	T > 1800

Isotropic Data

Thermal-conductivity data from references 4 and 6 were obtained on cermets in which the particles were essentially spherical in shape with concentrations between 50 and 70 volume percent. This range of conditions allowed the variable dispersion model (eq. (3)) to be applied directly in estimating the conductivity of the material. However, because of the fabrication method, the materials used for the measurements were not

TABLE II. - COMPOSITION AND DENSITY OF

CERMET MATERIAL USED IN THERMAL

CONDUCTIVITY COMPARISON

Material composition	Uranium dioxide particle concentration, vol. %	Density, percent of theoretical	Void fraction, percent
W-UO$_2$	50	92.5	7.5
W-UO$_2$	70	94.5	5.5
Mo-UO$_2$	60	94.0	6.0

fully densified. Table II lists the composition, density, and resulting void fraction for these materials.

A method that attempts to account for the nontheoretical density of these three materials is to calculate the thermal conductivity of the composite as though it were 100 percent dense. The resulting effective conductivity of the theoretically dense mixture is then used as the matrix conductivity, the conductivity of the voids is assumed to be negligible, and the calculation is repeated with the particle concentration now corresponding to the measured void fraction of the compacts (table II). When this method is applied to the variable dispersion model (eq. (3)), the effective thermal conductivity corrected for density variation can be expressed as

$$K_{eff,\rho} = K_{eff,\rho_0} \left(\frac{\rho}{\rho_0}\right)^{3/2} \tag{14}$$

where ρ and ρ_0 refer to the actual and theoretical density of the composite, respectively.

Figure 8 shows the comparison between the experimental results and the analytically predicted values of thermal conductivity. The long-dashed curve, shown as the theoretical density line, was obtained by applying the variable dispersion equation directly, and by assuming a fully dense material. The short-dashed curves are the result of correcting for the density variations of the three materials used in these experiments. Although the tungsten - uranium dioxide comparison appears to be much better than the molybdenum - uranium dioxide results, there is still reasonable agreement considering potential sources of experimental error and the scatter in the thermal conductivity data of the base materials used in the analysis (figs. 7(a) to (c)).
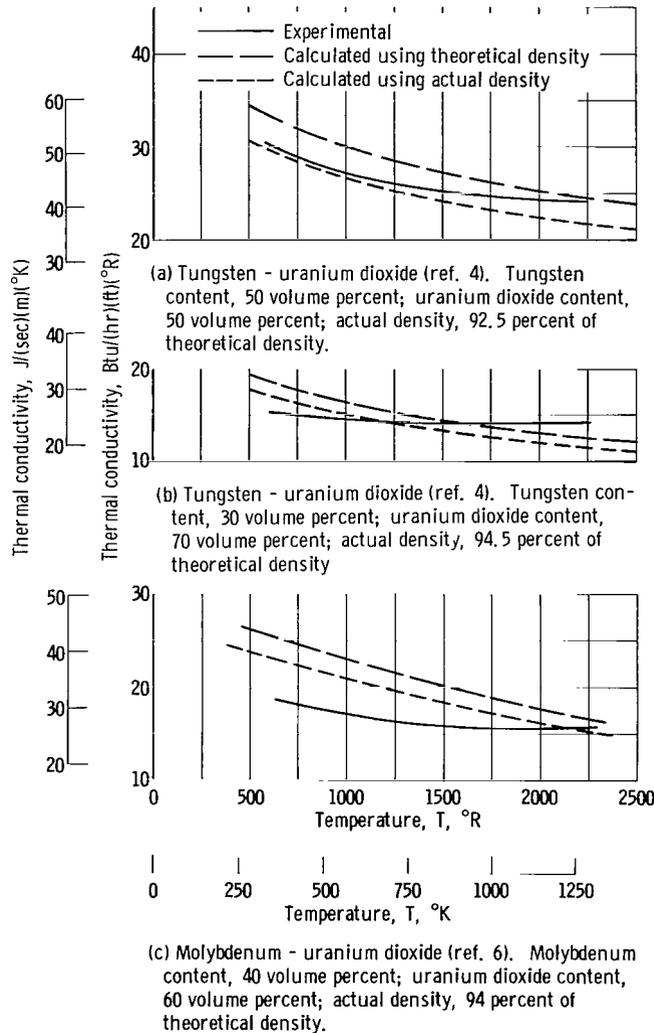
14

(a) Tungsten – uranium dioxide (ref. 4). Tungsten content, 50 volume percent; uranium dioxide content, 50 volume percent; actual density, 92.5 percent of theoretical density.

(b) Tungsten – uranium dioxide (ref. 4). Tungsten content, 30 volume percent; uranium dioxide content, 70 volume percent; actual density, 94.5 percent of theoretical density

(c) Molybdenum – uranium dioxide (ref. 6). Molybdenum content, 40 volume percent; uranium dioxide content, 60 volume percent; actual density, 94 percent of theoretical density.

Figure 8. – Comparison between experimental and predicted values of thermal conductivity of cermet fuel material.

Anisotropic Data

Reference 5 contains the experimental results of thermal-conductivity measurements made on tungsten – uranium dioxide dispersions with particle concentrations of from 10 to 40 volume percent. In these experiments, the conductivity was not measured directly but was obtained by the flash diffusivity method (ref. 17), in which the thermal conductivity is calculated from measurements of the specific heat, density, and thermal diffusivity.

$$K_t = \left(\alpha \rho C_p \right)_t \tag{15}$$
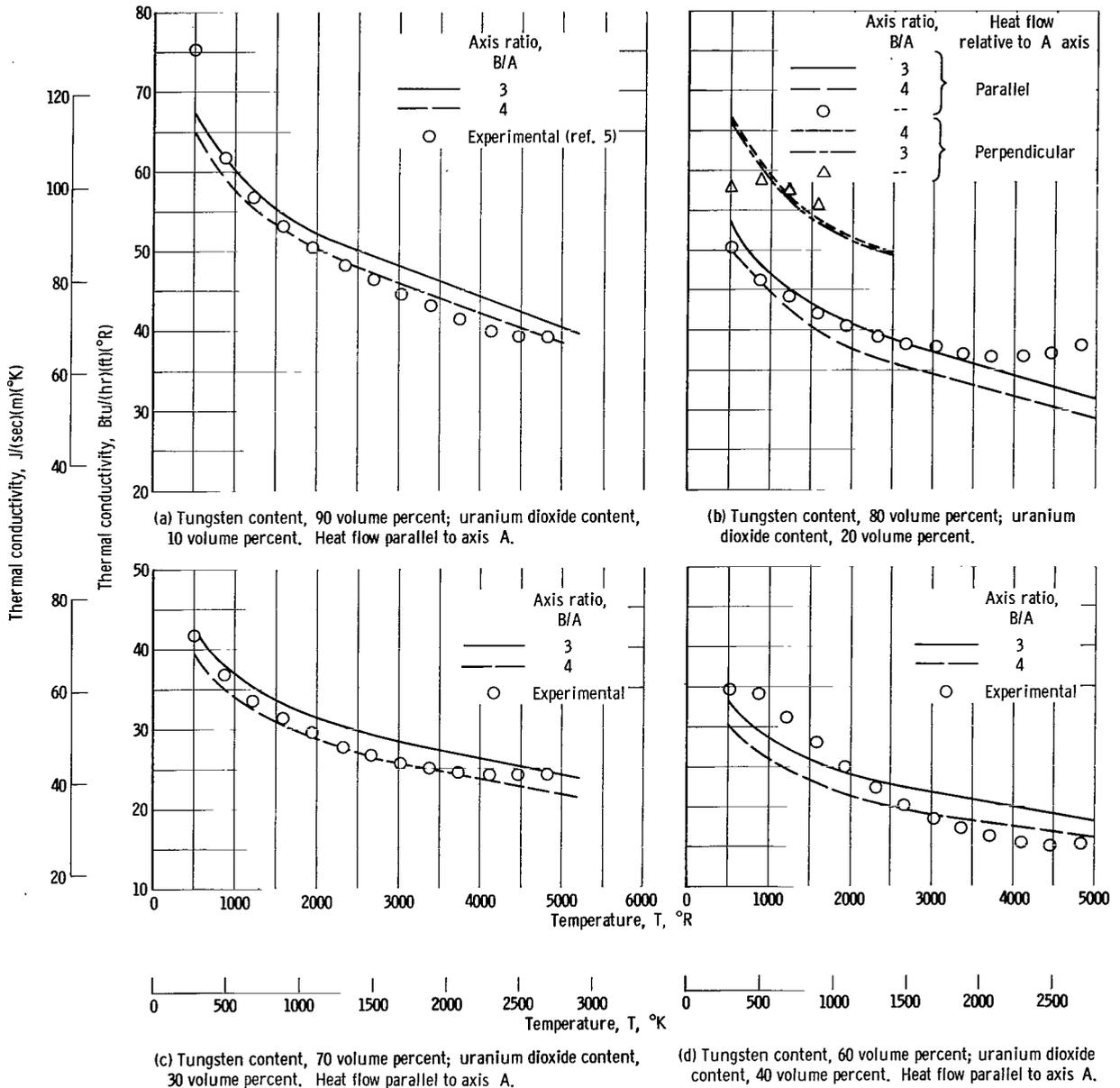
15

Figure 9. – Comparison of experimental and analytical values of thermal conductivity.

16

Parker (ref. 17) estimated that the flash diffusivity technique yields results that are within ±10 percent of previously established values. This appears to be consistent with Taylor's observations (ref. 5) that the error in measuring specific heat and density were from 3 to 4 percent each and that determination of the thermal diffusivity was accurate to about 2 percent.

The materials used by Taylor (ref. 5) to obtain the thermal conductivity data were manufactured by a rolling process and, although completely densified, the particles were distorted by the rolling operation. The resulting particle shape was not strictly an oblate ellipsoid, because the elongation of the particle in the rolling direction was four to six times the particle thickness and only two to three times the particle thickness in the direction perpendicular to the rolling direction. Because the analytical method of Fricke assumes that the two major axes are equal, the true solution to the anisotropic case for the above conditions is somewhere near the average, or a particle with a major to minor axis ratio of 3 or 4.

The results of the comparison between the measured thermal conductivity and that predicted by the suggested model (eq. (9)) is shown in figure 9. Agreement between the experimental and analytical values is quite good considering the assumptions made in selecting the mean-value conductivity of tungsten (fig. 7(a)) and uranium dioxide (fig. 7(c)) and the possible 10 percent experimental error associated with the flash diffusivity technique for obtaining the thermal conductivity. It would appear that the suggested method (eq. (9)) of correcting the variable dispersion equation by the anisotropic correction factor (eq. (7)) yields results which are within the experimental accuracy.

CONCLUDING REMARKS

There are at least three basic models (ref. 2) that appear to be satisfactory for estimating the thermal conductivity of cermet material:

(1) The dilute dispersion model (eq. (2))
(2) The variable dispersion model (eq. (3))
(3) The mixture model (eq. (4))

Available experimental data on tungsten - uranium dioxide (ref. 4) and molybdenum - uranium dioxide (ref. 6) dispersions have been compared with the thermal conductivity predicted by the appropriate model (eq. (3)). Considering the uncertainty in the thermal-conductivity value of the base materials, the results of the comparison were favorable. Similar comparisons on a wide variety of materials have also been successfully made by other investigators (ref. 2, p. 8).

In addition to the three basic models, anisotropic versions of the dilute dispersion model (eq. (5)) and the mixture model (eq. (8)) are also available. Because of the as-

sumptions made in the derivation of all these models, however, the range of applicability of each is limited and does not include all the regions that may be of interest for dispersion fuels. A suggested model for this undefined region is proposed by noting the similarity in the results obtained from the dilute dispersion models (eq. (2)) and the variable dispersion models (eq. (3)). The resulting equation for the effective thermal conductivity is given by

$$K_{eff(corrected)} = K_{(3)} \frac{K_{(5)}}{K_{(2)}} \tag{9}$$

where the subscripts refer to values obtained from equations (2), (3), and (5).

This method of correcting for anisotropic effects is semiempirical in nature, because there is no true mathematical basis for such a procedure. However, the suggested method, when compared with available experimental data (ref. 5), yields results that are within the expected range of experimental errors. It would, therefore, appear that this model can be used to predict successfully the thermal conductivity of potential fuel materials, at least for the preliminary phases of a nuclear reactor design. Comparison of the analytical values with future experimental data could extend the range of applicability and increase the confidence level in the use of the model.

With an argument similar to that used in formulating the anisotropic correction factor for the undefined region, a coating correction factor, applicable when the particles are coated with a third material, can also be defined so that the thermal conductivity of the composite material is given by

$$K_{eff} = K_{(3)} \left[\frac{K_{(5)}}{K_{(2)}} \right] \left[\frac{K_{(10)}}{K_{(2)}} \right] \tag{12}$$

where the subscripts again refer to the values obtained from the respective equations. While there are no experimental data presently available to verify this method, it is presented for possible future reference.

Lewis Research Center,
    National Aeronautics and Space Administration,
        Cleveland, Ohio, November 29, 1966,
            122-20-02-04-22.

APPENDIX A

SYMBOLS

A, B, C   axes of ellipsoid, ft (m)

a, b, c   curve fit coefficients in thermal conductivity expression (eq. (13))

C_p specific heat at constant pressure, Btu/(lb)(^{O}R) J/(kg)(^{O}K)

K   thermal conductivity, Btu/(hr)(ft)(^{O}R) J/(sec)(m)(^{O}K)

L   plate thickness, ft, (m)

M   function defined in appendix B

Q   heat generation rate, Btu/(hr)(cu ft)$\left(\text{J/(sec)(m}^3)\right)$

R   ratio of thermal conductivities, K_p/K_m

T   temperature, ^{O}R (^{O}K)

V   volume fraction

X   function defined in appendix B

α thermal diffusivity, sq ft/hr (m^2/sec)

β function defined in appendix B

γ ratio of mean field strengths

θ angle defined in appendix B

ρ density, lb/cu ft (kg/m^3)

φ angle defined in appendix B

Subscripts:

c   condition in coating

eff   effective value of mixture

m   condition in matrix

max   maximum value

o   theoretical value

p   condition in particle

t   evaluated at temperature T

w   condition at wall

APPENDIX B

EQUATIONS USED TO DETERMINE THERMAL CONDUCTIVITY
OF ANISOTROPIC DISPERSIONS

The original work done by Fricke, a biophysicist working on the electrical behavior of blood, was based on the random orientation of a dilute dispersion of ellipsoids. Power (ref. 2) shows how this work can be extended to two-directional preferred orientation. The result of this analysis is shown in the following equations that were used to determine the effective conductivity of anisotropic dispersions:

The dilute dispersion model is given by

$$\frac{K_{eff}}{K_m} = \frac{R(1 + XV_p) + X(1 - V_p)}{R(1 - V_p) + (X + V_p)} \tag{B1}$$

(Note that this is an alternate form of eq. (5).)

The mixture model is

$$\frac{K_m - K_{eff}}{K_m + XK_{eff}} = \frac{V_p}{1 - V_p} \frac{K_{eff} - K_p}{K_p + XK_{eff}} \tag{B2}$$

where

$$X = \frac{R(\beta - 1) + 1}{R - (\beta + 1)} \tag{B3}$$

and

$$R = \frac{K_p}{K_m}$$

The values of β for various conditions are as follows:

For the A axis oriented parallel to the heat flux

$$\beta = \frac{R - 1}{1 + (R - 1)(1 - M)} \tag{B4}$$

For the A axis oriented perpendicular to the heat flux

$$\beta = \frac{R - 1}{1 + (R - 1)\dfrac{M}{2}}$$ (B5)

For random orientation

$$\beta = \frac{R - 1}{3}\left[\frac{2}{1 + (R - 1)\dfrac{M}{2}} + \frac{1}{1 + (R - 1)(1 - M)}\right]$$ (B6)

where, for $A < B$

$$M = \left(\frac{\theta - \dfrac{1}{2}\sin 2\theta}{\sin^3 \theta}\right)\cos \theta$$ (B7)
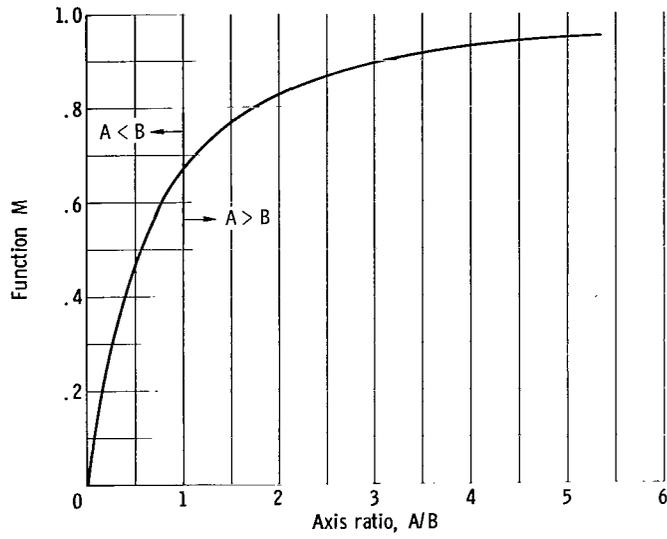
and

$$\cos \theta = \frac{A}{B}$$

and, for $A > B$,

$$M = \frac{1}{\sin^2 \varphi} - \frac{1}{2}\left(\frac{\cos^2 \varphi}{\sin^3 \varphi}\right)\log_e\left(\frac{1 + \sin \varphi}{1 - \sin \varphi}\right)$$ (B8)

and

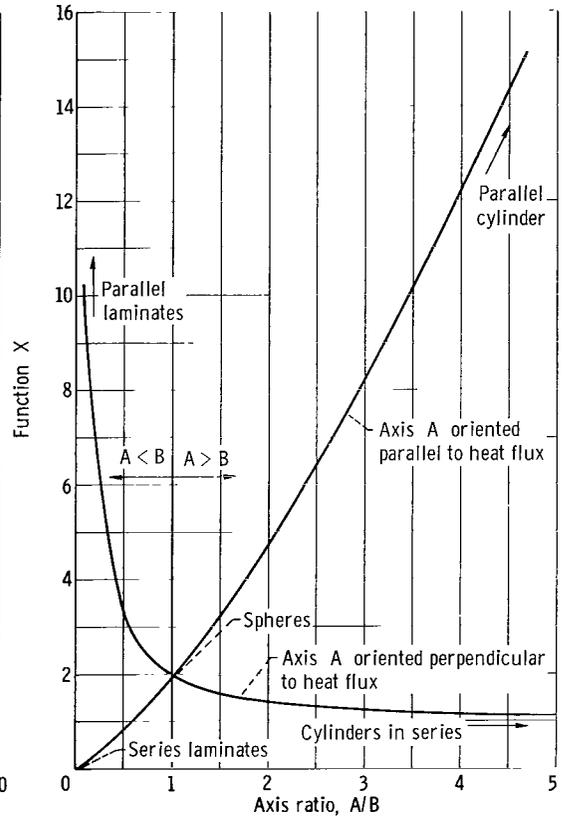$$\cos \varphi = \frac{B}{A}$$

The variation of M, β, and X is shown in figure 10 for several conditions.

(a) Function M.
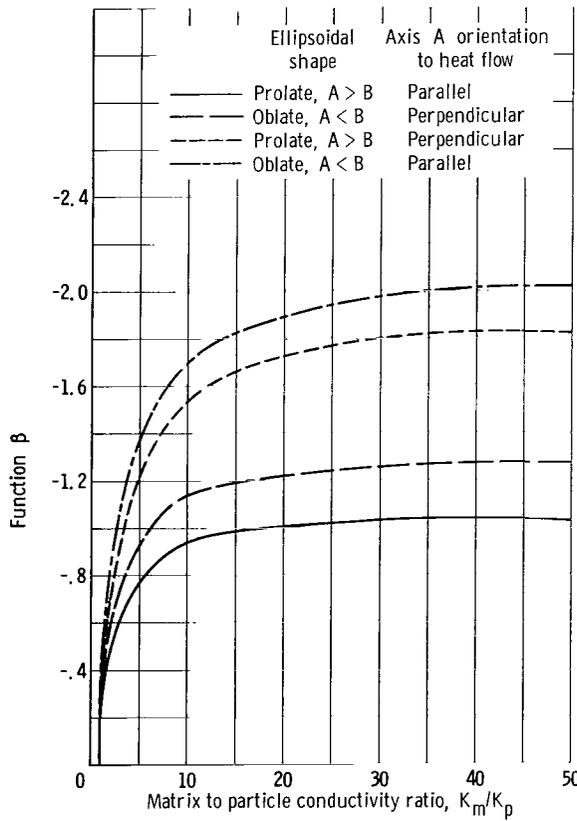
(b) Function β; major-minor axis ratio, 5.

(c) Function X.

Figure 10. - Variation of functions with particle shape, orientation, and elongation.

APPENDIX C

VARIATION OF THERMAL CONDUCTIVITY OF TUNGSTEN - URANIUM

DIOXIDE DISPERSIONS

To illustrate the thermal conductivity behavior of cermet fuels under various conditions, calculations were performed for a range of compositions of tungsten - uranium dioxide dispersions. Figures 11 to 15 summarize the results of this investigation. The values were calculated by using the suggested method described in the text (eq. (9)) and utilizing the mean value of thermal conductivity for the two base materials (figs. 7(a) and (c), p. 12). Except for figures 12 and 13, all the values were calculated by using oblate ellipsoids where axis $A < B = C$.
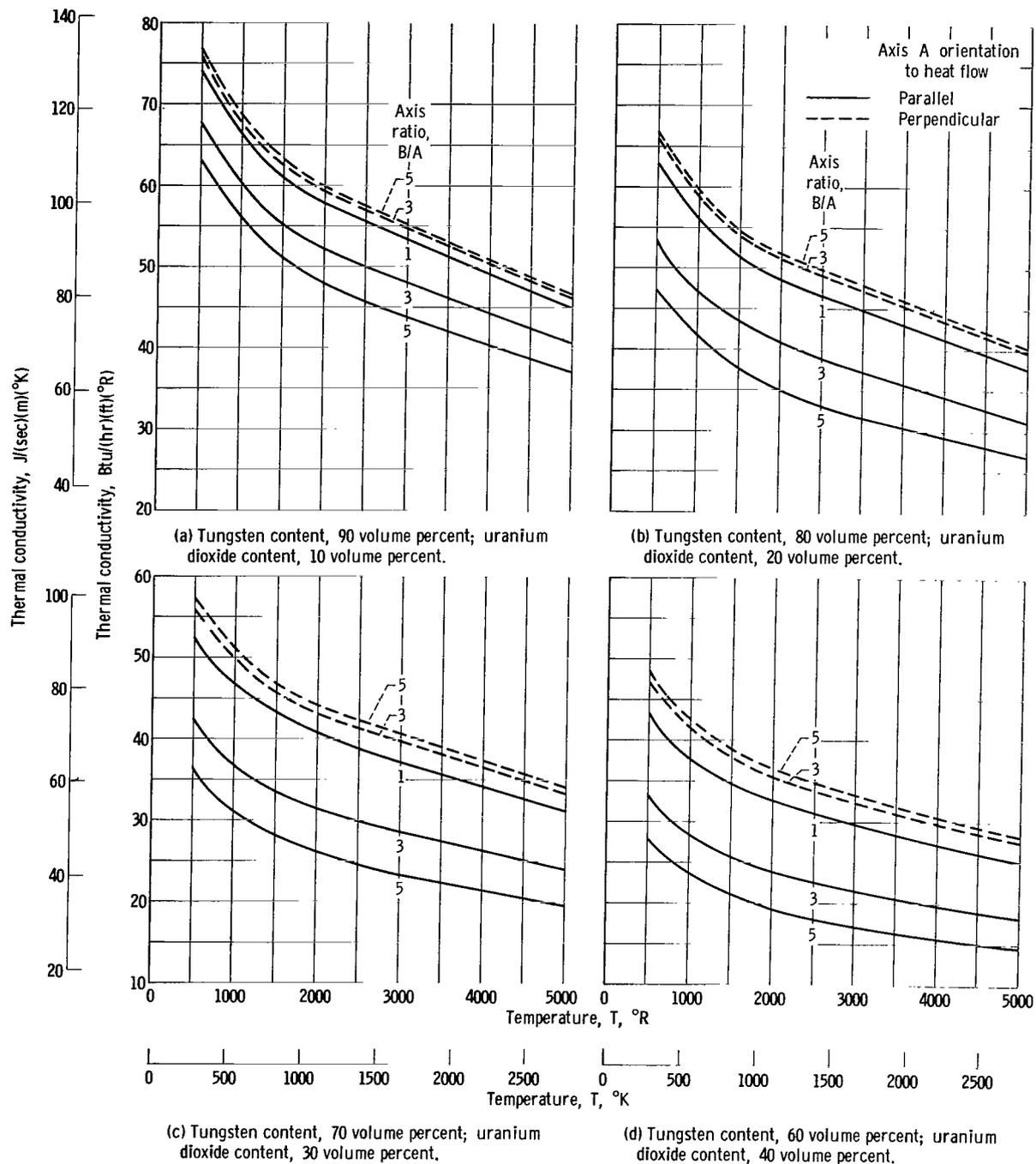
(a) Tungsten content, 90 volume percent; uranium dioxide content, 10 volume percent.

(b) Tungsten content, 80 volume percent; uranium dioxide content, 20 volume percent.

(c) Tungsten content, 70 volume percent; uranium dioxide content, 30 volume percent.

(d) Tungsten content, 60 volume percent; uranium dioxide content, 40 volume percent.

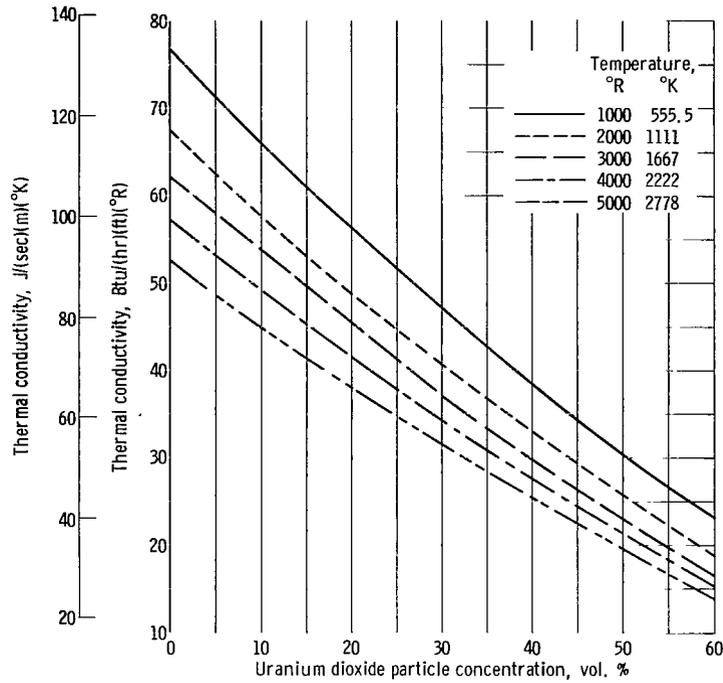Figure 11. - Effect of particle elongation on thermal conductivity of tungsten-uranium dioxide dispersions.

Figure 12. – Effect of temperature on thermal conductivity of
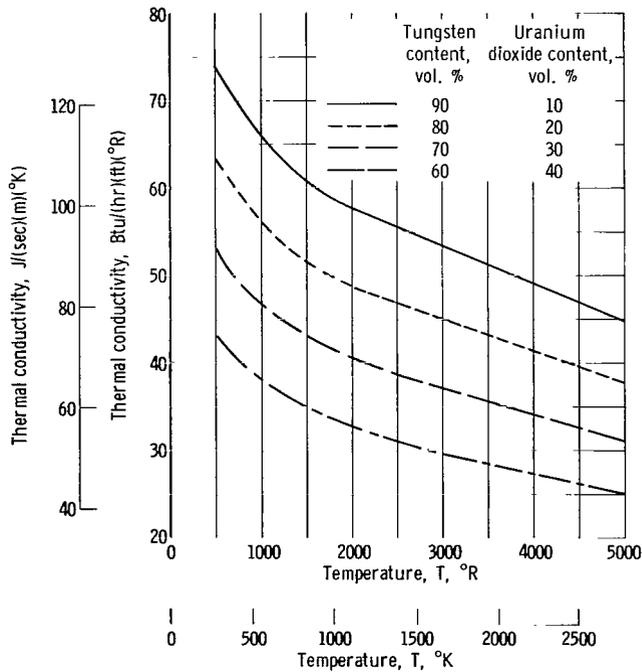tungsten-uranium dioxide dispersions for spherical particles.

Figure 13. – Effect of particle concentration on thermal
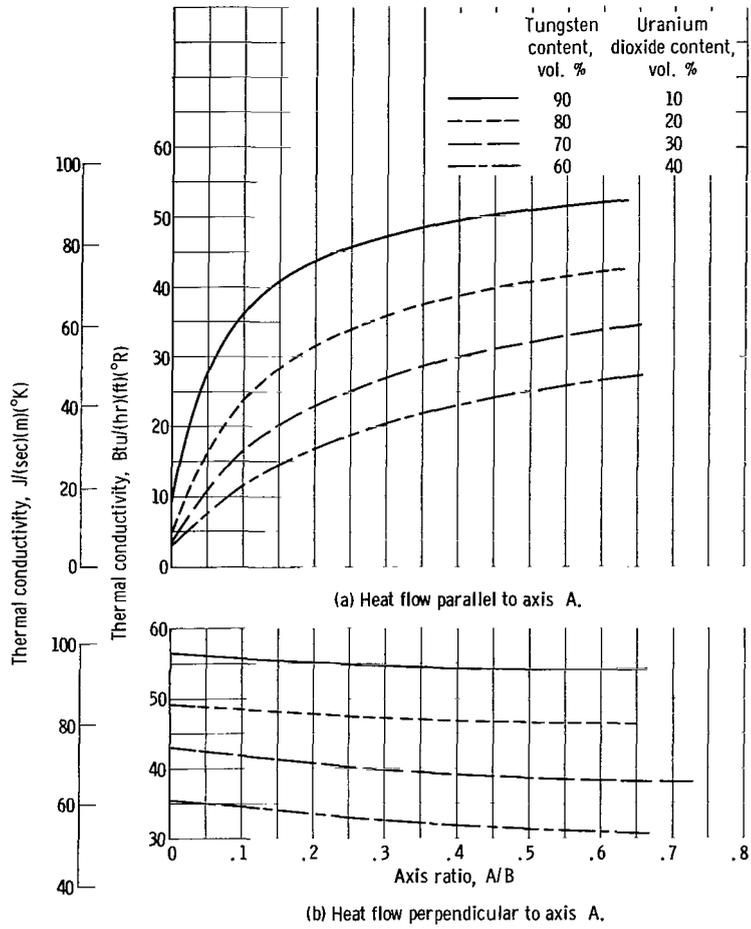conductivity of tungsten-uranium dioxide for spher-
ical particles.

25

(a) Heat flow parallel to axis A.

(b) Heat flow perpendicular to axis A.

Figure 14. - Effect of axis ratio on thermal conductivity of tungsten-uranium dioxide dispersions. Temperature, 3000° R (1667° K).
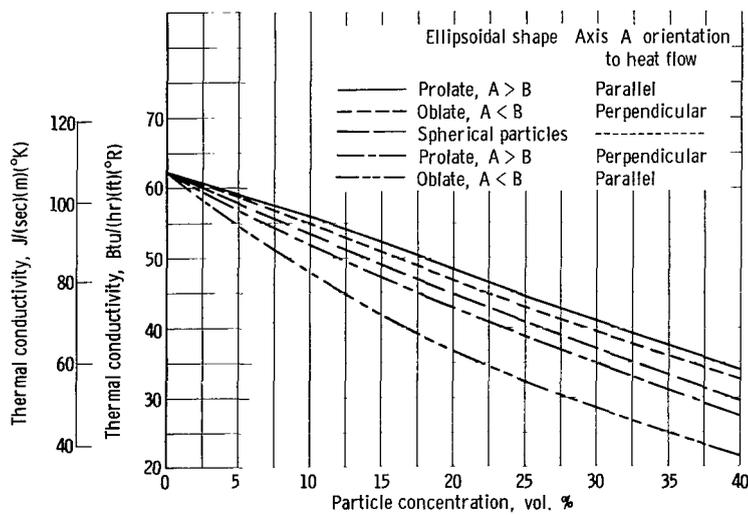

Figure 15. - Effect of particle shape and orientation on thermal conductivity of tungsten-uranium dioxide dispersions. Temperature, 3000° R (1667° K); major to minor axis ratio, 3.

26

REFERENCES

1. Miller, John V.: Predicting Thermal Conductivity of Tungsten - Uranium Dioxide Dispersions. NASA TM X-1145, 1965.

2. Powers, A. E.: Conductivity in Aggregates. Rept. No. KAPL-2145, Knolls Atomic Power Lab., General Electric Co., Mar. 6, 1961.

3. Brown, George G.: Unit Operations. John Wiley & Sons, Inc., 1950, p. 215.

4. Dayton, Russell W.; and Dickerson, Ronald F.: Progress Relating to Civilian Applications During February 1963. Rept. No. BMI-1619, Battelle Memorial Inst., Mar. 1, 1963.

5. Taylor, R. E.: Thermal Properties of Tungsten-Uranium Dioxide Mixtures. Rep. No. AI-64-153 (NASA CR-54141), Atomics International, Sept. 1, 1964.

6. Dayton, Russell W.; and Dickerson, Ronald F.: Progress Relating to Civilian Applications During April 1963. Rept. No. BMI-1630, Battelle Memorial Inst., May 1, 1963.

7. Anon.: Tungsten. Metallwerk Plansee (Austria), 1963.

8. Schmidt, F. F.; and Ogden, H. R.: The Engineering Properties of Tungsten and Tungsten Alloys. Rept. No. DMIC-191, Battelle Memorial Inst., Sept. 27, 1963.

9. Anon.: How Tungsten Does It Better. Bull. No. MI-5301, Fansteel Metallurgical Corp., 1963.

10. Goldsmith, Alexander; Waterman, Thomas E.; and Hirschorn, Harry J.: Thermophysical Properties of Solid Materials. Vol. I - Elements. (WADD TR 58-476, vol. 1), Armour Research Foundation, Aug. 1960.

11. Hogerton, J. F.; and Grass, R. C., eds.: General Properties of Materials, The Reactor Handbook. Vol. 3 - Materials. Sec. 1 - General Properties. AECD-3647, AEC, Mar. 1965.

12. Weiss, V.; and Sessler, J. G., eds.: Non-Ferrous Alloys. Vol. II of Aerospace Structural Metals Handbook. Syracuse University Press, 1963.

13. Rasor, N. S.; and McClelland, J. D.: Thermal Properties of Materials. Part 1 - Properties of Graphite, Molybdenum and Tantalum to Their Destruction Temperatures. (WADC-TR 56-400, pt. 1), Atomics International, Mar. 1957.

14. Mikol, Edward P.: The Thermal Conductivity of Molybdenum Over the Temperature Range 1000 - 2100° F. Rep. No. ORNL-1131, Oak Ridge National Laboratory, Feb. 28, 1952.

15. Cottrell, W. B.; Culver, H. N.: Scott, J. L.; and Yarosh, M. M.: Fission-Product Release From UO_2. Rep. No. ORNL-2935, Oak Ridge Nat. Lab., Sept. 13, 1960.

16. Belle, Jack, ed.: Uranium Dioxide: Properties and Nuclear Applications. AEC, 1961.

17. Parker, W. J.; Jenkins, R. J.; Butler, C. P.; and Abbott, G. L.: Flash Method of Determining Thermal Diffusivity, Heat Capacity, and Thermal Conductivity. J. Appl. Phys. vol. 32, no. 9, Sept. 1961, pp. 1679-1684.

NASA SCIENTIFIC AND TECHNICAL PUBLICATIONS

TECHNICAL REPORTS: Scientific and technical information considered important, complete, and a lasting contribution to existing knowledge.

TECHNICAL NOTES: Information less broad in scope but nevertheless of importance as a contribution to existing knowledge.

TECHNICAL MEMORANDUMS: Information receiving limited distribution because of preliminary data, security classification, or other reasons.

CONTRACTOR REPORTS: Technical information generated in connection with a NASA contract or grant and released under NASA auspices.

TECHNICAL TRANSLATIONS: Information published in a foreign language considered to merit NASA distribution in English.

TECHNICAL REPRINTS: Information derived from NASA activities and initially published in the form of journal articles.

SPECIAL PUBLICATIONS: Information derived from or of value to NASA activities but not necessarily reporting the results of individual NASA-programmed scientific efforts. Publications include conference proceedings, monographs, data compilations, handbooks, sourcebooks, and special bibliographies.

Details on the availability of these publications may be obtained from:

SCIENTIFIC AND TECHNICAL INFORMATION DIVISION

NATIONAL AERONAUTICS AND SPACE ADMINISTRATION

Washington, D.C. 20546